

# ASSESSMENT OF LOAD HISTORY EFFECTS ON FRACTURE

P J Budden  
British Energy Generation  
Barnett Way, Barnwood  
Gloucester, GL4 3RS, UK  
email: peter.budden@british-energy.com

D C Connors  
BNFL Magnox Generation  
Berkeley  
Gloucestershire, GL13 9PB, UK  
email: d.connors@magnox.co.uk

## Abstract

The fracture toughness is a key materials data requirement for practical defect assessments of engineering plant. However, the apparent toughness or load to fracture can be affected by the history of loading. For example, prior loads due to proof pressure tests (PPT) or warm pre-stress (WPS), and sustained loading (cold creep) may all have an effect. Moderate levels of appropriate PPT or WPS loading are generally considered to improve the subsequent apparent toughness properties, whereas, in the susceptible temperature and stress range, time-dependent crack growth can occur under sustained loading.

In this paper, WPS data on ferritic steels are compared with the predictions of simplified models. The analyses validate forthcoming revised advice within the R6 defect assessment procedure. Furthermore, recent studies within the R6 development programme leading to updated advice on the treatment of the PPT and sustained loads are also briefly described.

## Introduction

Structural integrity assessments of engineering plant containing crack-like defects, using fitness-for-service procedures such as R6 [1], require the material's fracture toughness,  $K_{mat}$ , as an input parameter. The chosen value of toughness should be relevant to the material at the crack tip, in the assessed condition and at the relevant temperature  $K_{mat}$  is compared with an estimate of the crack driving force, either directly using a parameter such as the stress intensity factor,  $K$ , or the  $J$ -integral, or indirectly using a failure assessment diagram (FAD). However, the apparent toughness or load to fracture can be affected by the history of loading. This paper considers a number of potential load history scenarios which may need to be taken into account in a practical plant assessment. The main content of the paper is concerned with the warm pre-stress (WPS) effect. The WPS effect is described more fully later in the paper. Models for the quantification of the beneficial enhancement in the value of  $K_{mat}$  due to WPS are discussed, validation of the models using WPS test data is described, and developments in the advice for their treatment within R6 outlined. Recent work within the R6 development programme leading to revised advice on the treatment of the proof pressure test (PPT) and of sustained loading (cold creep) effects on load to fracture are then also briefly discussed.

## The Warm Prestress Effect

A WPS is an initial pre-load applied to a ferritic structure containing a pre-existing flaw which is carried out at a temperature above the ductile-brittle transition temperature, and at a higher temperature or in a less-embrittled state than that corresponding to the subsequent service assessment. A WPS argument confers added resistance to fracture under the assessment conditions. That is, a WPS is considered to elevate the stress intensity factor at fracture,  $K_f$ , above the corresponding fracture toughness,  $K_{mat}$ , in the absence of the WPS [2-14]. In service assessments, the fracture toughness is then taken as  $K_f$ . In the laboratory, there are three basic types of WPS cycle which are used to demonstrate the WPS effect (Figure 1):

- Load-Unload-Cool-Fracture (LUCF), where the structure is pre-loaded at temperature  $T_1$  to stress intensity factor  $K_1$ , unloaded to stress intensity factor  $K_2$ , cooled to temperature  $T_2$  and re-loaded to fracture.
- Load-Cool-Unload-Fracture (LCUF), where cooling to  $T_2$  takes place prior to unloading and re-loading to fracture.
- Load-Cool-Fracture (LCF). This is similar to the LCUF cycle except that no unloading occurs prior to the imposition of extra load to fracture.

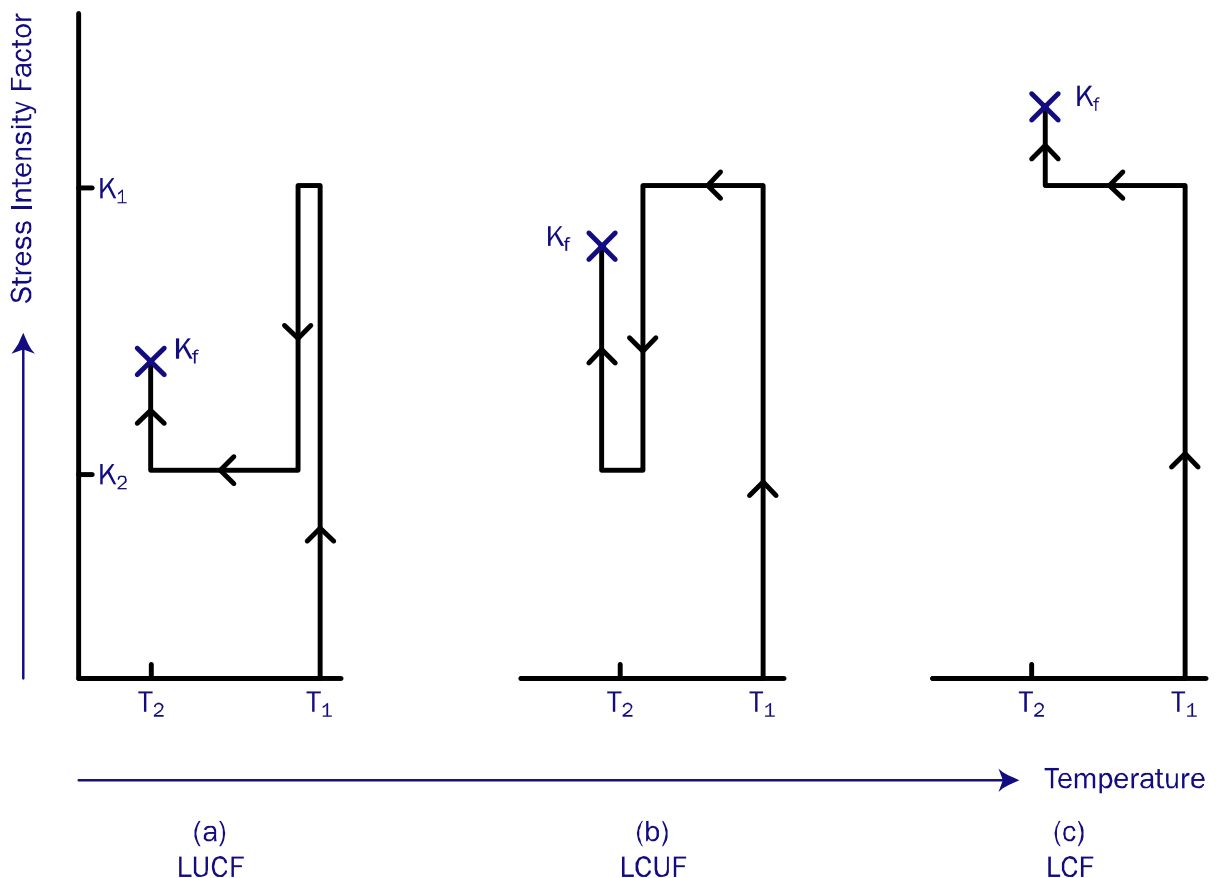


FIGURE 1. Typical laboratory WPS cycles

The greatest benefit in terms of maximising  $K_f$  is given by the LCF cycle, the least by the LUCF cycle with full unloading. Intermediate forms of cycle, where partial unloading occurs prior to re-loading to failure, and where the temperature and pressure are simultaneously reduced, give benefits lying between these two limits.

For a WPS argument to be made, the following conditions are normally considered necessary.

- (i) The failure mechanism at the service condition is transgranular cleavage or intergranular brittle fracture [2,7].
- (ii) The flow properties of the material increase between the WPS and the service failure condition (due to a decrease in temperature or due to in-service hardening).
- (iii) There is no significant sub-critical crack growth between the WPS and the service failure condition. The amount of any such crack growth should be much less than the extent of the residual plastic zone following unloading [11].
- (iv) The stress intensity factor,  $K_1$ , due to the WPS loading exceeds the fracture toughness,  $K_{mat}$ , at the re-load condition.
- (v) Small-scale yielding conditions hold at the pre-load. There is evidence [5] that, for increasing pre-loads, the benefits on the apparent re-load fracture toughness lessen. Indeed, in the limit of extensive plasticity, the toughness may actually be reduced compared to its value in the absence of the WPS.
- (vi) The pre-load and re-load should be in the same direction; that is, both tensile or both compressive at the crack tip. A compressive pre-load followed by a tensile re-load may reduce the apparent fracture toughness.

The benefits of a WPS in thick-section components have been attributed [2] mainly to the establishment of a compressive residual stress zone ahead of the crack tip. However, generally, the effects of crack-tip blunting and strain hardening have also been claimed as significant by a number of authors. Experimental demonstration of the WPS effect has been reported in many references using both small specimen and feature tests. A number of alternative quantitative models of WPS benefits have been developed, both ‘global’ models based on crack driving force [3-5] and energetic [12] considerations, and ‘local’ models [2,13-14] which use local approach methods. Validation of the model predictions against both specimen and large-scale test data is summarised in, for example, [2,10].

The current issue of R6 restricts the application of WPS to transgranular cleavage fracture, consistent with the conclusions of the review by the UK Technical Advisory Group on Structural Integrity (TAGSI) [7]. However, it has been argued [2] that this restriction is unnecessary and that a WPS benefit both exists in the case of failure by stress-controlled intergranular brittle fracture mechanisms and may also be quantified using existing WPS models. There is experimental evidence for this assertion [2,9]. Hence the restriction on fracture mode is being relaxed at the next amendment to R6.

### ***Simplified Models***

There are a number of published quantitative models of the WPS effect [3-6,8,12]. In particular, Chell & Haigh [3] simplified Chell’s alternative more complex model for situations most relevant to the LUCF cycle. A similar simplified expression for  $K_f$  was also

given by Smith & Garwood [6]. These last two models are currently set down in R6 [1]. The expression in [3] is

$$K_f = K_2 + 0.2\Delta K_u + 0.87K_{mat} \quad (1)$$

provided that the re-load  $K_f - K_2 \leq (1 + \lambda)\Delta K_u / 2$ , where  $\Delta K_u = K_1 - K_2$  and  $\lambda \geq 1$  is the ratio of the flow stresses at the re-load and pre-load temperatures. Otherwise,  $K_f = \max(K_2, K_{mat})$  is assumed. Conservatively,  $\lambda=1$  is used in the following analyses.

Recently, Wallin [8] has derived eqn.(2) below, which represents an interpolation between expressions for the bounding cases of LUCF with full unloading and the LCF cycle. The stress intensity factor at failure follows from

$$K_f = K_2 + \sqrt{K_{mat}\Delta K_u} + 0.15K_{mat} \quad (2)$$

when  $K_{mat} < \Delta K_u$ . If  $K_{mat} \geq \Delta K_u$ , then the conditions  $K_2 = K_1$  and  $\Delta K_u = 0$  are imposed in eqn.(2). If the calculated  $K_f \leq K_{mat}$  then no WPS benefit is estimated and  $K_f = K_{mat}$  is assumed.

### Test Data

WPS test data on a French reactor pressure vessel steel, 18MND5, similar to SA533B, have been obtained by Electricit  de France (EDF) within the European project SMILE [15]. The chemical composition of the steel is given in Table 1. Conventional fracture toughness tests were conducted by SMILE partners, over the temperature range  $-196^\circ\text{C}$  to  $20^\circ\text{C}$ , using compact tension (CT) specimens with crack length to specimen width ratios between 0.48 and 0.56. The fracture toughness of the material was described by the Master Curve [16] approach with a reference temperature  $T_0 = -97^\circ\text{C}$ . Hence the median and 5% cleavage fracture toughness values at the re-load temperature of  $-150^\circ\text{C}$  are  $55.6\text{MPa}\sqrt{\text{m}}$  and  $38.6\text{MPa}\sqrt{\text{m}}$ , respectively. A series of WPS tests were also performed on 1CT and 2CT specimens under a variety of load histories, where  $K_1 \cong 60\text{MPa}\sqrt{\text{m}}$  or  $100\text{MPa}\sqrt{\text{m}}$ . These included LCF and LUCF ( $K_2 = 0$ ) cycles, cases where the temperature and load reduced simultaneously prior to re-load to fracture with  $K_2 = K_1 / 2$  (LTF), and cases where the load level experienced small oscillations during cooling, with  $K_2 = K_1$  (LOCF) or  $K_2 = K_1 / 2$  (LOTF). All tests failed by cleavage. The test data will be analysed by the SMILE partners using a number of global and local models of fracture. The analysis of the data using eqns. (1)-(2) is given below. The oscillations in the LOTF and LOCF tests are neglected.

TABLE 1. Chemical composition of 18MND5 steel (wt %)

C	Mn	Si	Ni	Cr	Mo	Cu	S	P	Al	V
0.19	1.5	0.23	0.66	0.17	0.485	0.084	<0.001	0.004	0.011	0.004

Additional experimental WPS data are given by Kordisch et al. [17] and Stöckl et al. [18] and also analysed below. Tests on 22NiMoCr3-7 weld metal specimens were reported in [17] using a number of different load and temperature histories. Stöckl et al. [18] performed a number of LCF and LUCF tests on specimens of 10MnMoNi5-5 shape-welded steel using three-point bend specimens. In each case, the lowest measured value of  $K_{mat}$  is used in the following subsection, consistent with the use of a ‘lower bound’ value of material fracture resistance in fitness-for-service assessments.

### Analysis of Test Data

The predicted values of  $K_f$  from the SMILE tests [15], using the 5% value of  $K_{mat}$  within the Chell & Haigh [3] and Wallin [8] models, are shown in Figure 2, normalised by the test value of  $K_f$ . It can be seen that the Chell & Haigh [3] model is conservative. The Wallin [8] model is also generally conservative, but of reduced extent. Similar conclusions hold using the median value of toughness, but the conservatism is reduced.

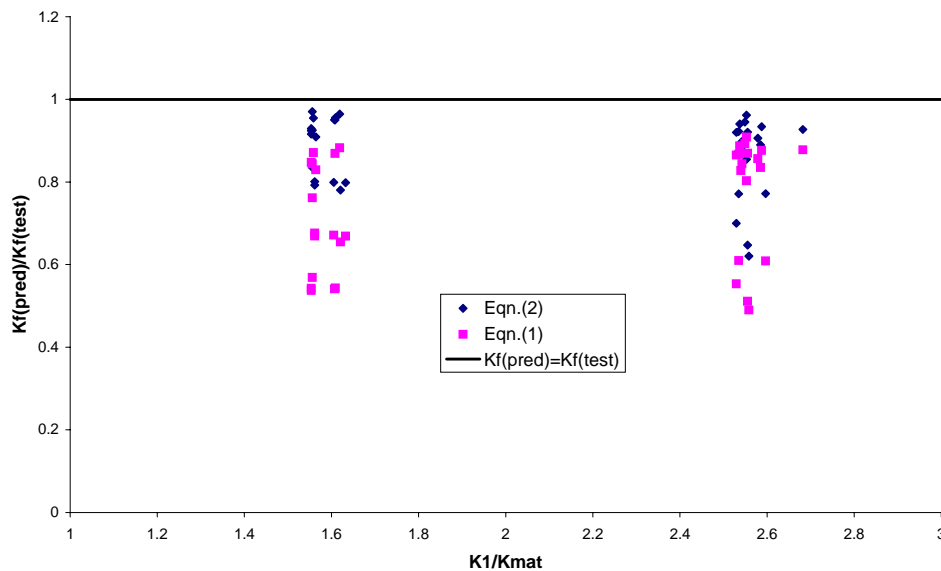


FIGURE 2. The SMILE [15]WPS data on 18MND5 (based on lower bound  $K_{mat}$ )

The LCF tests of Kordisch et al. [17] and Stöckl et al. [18] all showed that the stress intensity factor at fracture,  $K_f$ , was both greater than the fracture toughness and greater than the pre-load level of stress intensity factor. This is consistent with the conservative WPS principle, which says that failure will not occur under constant or falling load following the WPS (Figure 3). The predictions of eqn. (2) and the experimental results are shown in Figure 3, normalised by the measured toughness. The predictions are conservative in three of the five cases, and within about 1% of the test figure in the other two.

The test data from [17-18] involving unloading are shown in Figure 4. In all cases,  $K_f$  significantly exceeds the fracture toughness,  $K_{mat}$ , at the test temperature when the specimen had received a WPS pre-load. The predictions of eqn. (2) are generally pessimistic.

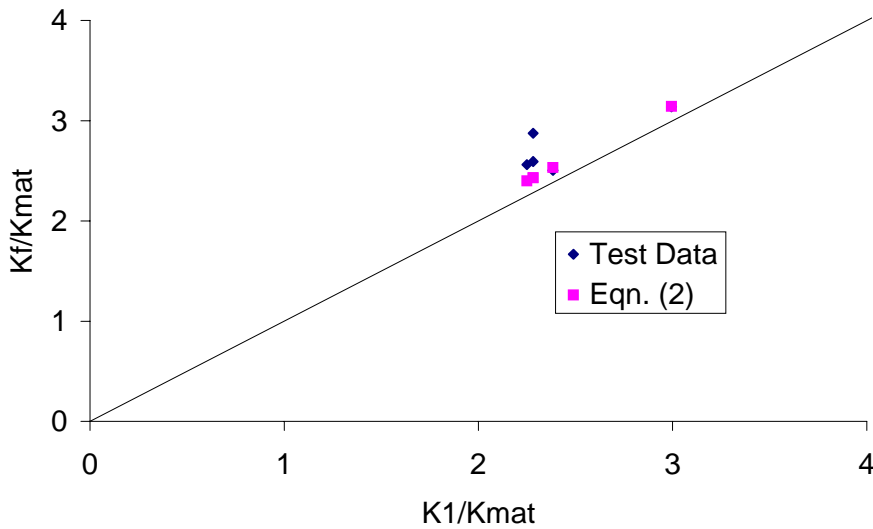


FIGURE 3 The LCF data [17-18] (based on lower bound  $K_{mat}$ )

In a few cases, the results are slightly non-conservative with the predicted value of  $K_f$  exceeding the measured value by up to 6%. The values of  $K_f$  calculated according to the simplified expression of eqn.(1) are also shown in Figure 4. These are consistently conservative. In some cases, the validity limits of eqn.(1) are not satisfied so that the values of  $K_f$  are given by  $K_f = \max(K_2, K_{mat})$ . Equation (2) predicts generally increased values of  $K_f$  compared with eqn.(1).

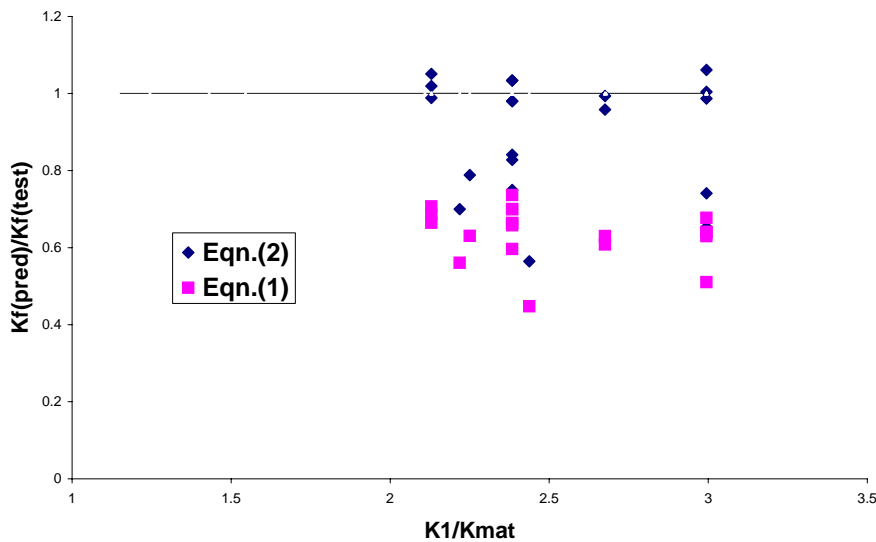


FIGURE 4. The WPS data with unloading [17-18] (based on lower bound  $K_{mat}$ )

## Discussion

As stated earlier, Section III.10 of R6 [1] covering WPS and PPT effects is about to be re-issued. This has modified and updated the advice on both these load history effects. The advice on PPT, which is not described in this paper, has been revised following a recent review by TAGSI in the UK. Apart from a general updating, it now includes a description of how the PPT can be used to infer a lower-bound value of toughness. The other load history phenomenon to be mentioned here is sustained loading. This is sometimes called ‘cold creep’ or ‘time-dependent plasticity’ and is addressed in Section III.4 of R6. Following the completion of an extensive experimental programme leading to uniaxial and CT sustained load data on Type 316L(N) austenitic steel [19], it was concluded that time-dependent plasticity effects need only be considered for austenitic steels for loads in excess of yield and at temperatures below 200°C. This corresponds to the regime where the stress-strain properties depend on loading rate. Beyond yield, strain could then accumulate with time at constant load. However, sufficient strain to lead to fracture only accumulated in the smaller CT specimens, which were close to  $J$ -instability on load-up and where only about 1 mm crack growth was required. In the larger CT specimens, and hence in structures, crack growth would be insufficient to lead to failure. The tolerance of the component to small amounts of crack growth would then need to be assessed. A method [1] based on the use of time-dependent, constant load uniaxial strain data has successfully assessed the fracture of the CT specimens. This work will be reported elsewhere.

## Summary

Advice on the treatment of load-history effects on fracture is given in the R6 defect assessment procedure [1]. This includes WPS, proof tests and sustained load effects. The current version of R6 recommends the simplified models of Chell & Haigh [3] and Smith & Garwood [6] for quantitative WPS assessments. Revised advice will be issued shortly which is based on the Wallin model [8]. This has an improved range of validity and is generally less pessimistic. This forthcoming revision of R6 also updates the advice on proof pressure tests (PPT), based on the recent review of TAGSI.

## Acknowledgements

This paper is published by permission of British Energy Generation and BNFL Magnox Generation. The data on 18MND5 steel were generated within the European Union Fifth Framework Project SMILE. The permission of the SMILE partners, in particular EDF, to publish the test data is gratefully acknowledged.

## References

1. R6: Assessment of the integrity of structures containing defects, Revision 4, Amendment 2, British Energy, Gloucester, 2003.
2. Smith, D. J., In *Comprehensive Structural Integrity*, Volume 7, Chapter 8, Elsevier, Oxford, 2003, 289-345.
3. Chell, G. G. and Haigh, J. R., *Int. J. Pres. Ves. Piping*, vol. **23**, 121-132, 1986.

4. Chell, G. G., In *Proceedings of the Fourth International Conference on Pressure Vessel Technology*, vol.1, 1980, 117-124.
5. Chell, G. G. and Curry, D. A., In *Developments in Fracture Mechanics-2*, edited by G. G. Chell, Applied Science, London, 1981, 161-177.
6. Smith, D. J. and Garwood, S. J., *Int. J. Pres. Ves. Piping*, vol. **41**, 333-357, 1990.
7. Burdekin, F. M. and Lidbury, D. P. G., *Int. J. Pres. Ves. Piping*, vol. **76**, 885-890, 1999.
8. Wallin, K., *Engng Fract. Mech.*, vol. **70**, 2587-2602, 2003.
9. Cheng, J. and Noble, F. W., *Fatigue Fract. Engng Mater. Struct.*, vol. **20**, 1399-1411, 1997.
10. Lidbury, D. P. G., Sherry, A. H., Pugh, C. E. and Bass, B. R., In *Comprehensive Structural Integrity*, Volume 7, Chapter 14, Elsevier, Oxford, 2003, 529-566.
11. Chell, G. G., *Fatigue Fract. Engng Mater. Struct.*, vol. **9**, 259-274, 1986.
12. Wadier, Y. and Bonnamy, M., In *Proceedings of ASME Pressure Vessels and Piping Conference*, Cleveland, vol. 461, ASME, New York, 2003, 89-96.
13. Pineau, A., In *Comprehensive Structural Integrity*, Volume 7, Chapter 5, Elsevier, Oxford, 2003, 177-225.
14. Beremin, F. M., In *Proceedings of the Fifth International Conference on Fracture (ICF5)*, 1981, 823-832.
15. Moinereau, D., Bezdikian, G. et al., In *Proceedings of the Eleventh International Conference on Nuclear Engineering*, Tokyo, JSME, 2003.
16. American Society for Testing and Materials, E1921-02, In *Annual Book of ASTM Standards*, vol. 03.01, 2003, 1128-1147.
17. Kordisch, H., Bösch, R., Blauel, J. G. Schmitt, W. and Nagel, G., *Nucl. Engng Design*, vol. **198**, 89-96, 2000.
18. Stöckl, H. Bösch, R., Schmitt, W., Varfolomeyev, I. and Chen, J. H., *Engng Fract. Mech.*, vol. **67**, 119 – 137, 2000.
19. Wardle, G., Birkett, R. P. and Budden, P. J., In *Proceedings of the Eleventh European Conference on Fracture (ECF11)*, vol.2, Poitiers-Futuroscope, France, 1996, 825-830.